Published in final edited form as:
*Brain Res*. 2013 May 28; 1512: 97–105. doi:10.1016/j.brainres.2013.03.033.

# High-Fat Diet Feeding Causes Rapid, Non-apoptotic Cleavage of Caspase-3 in Astrocytes

**Stephan J. Guyenet**[a], **Hong T. Nguyen**[a], **Bang H. Hwang**[a,b], **Michael W. Schwartz**[a], **Denis G. Baskin**[a,b], and **Joshua P. Thaler**[a]

Stephan J. Guyenet: guyenet@uw.edu; Hong T. Nguyen: hongtng@uw.edu; Bang H. Hwang: bhhwang@uw.edu; Michael W. Schwartz: mschwart@uw.edu; Denis G. Baskin: baskindg@uw.edu; Joshua P. Thaler: jpthaler@uw.edu

[a]Department of Medicine, Division of Metabolism, Endocrinology and Nutrition; Diabetes and Obesity Center of Excellence; University of Washington, Seattle, Washington, USA. UW medicine at South Lake Union, 850 Republican St, Box 358055, Seattle, WA 98109 USA

[b]Office of Research and Development, Department of Veterans Affairs Puget Sound Health Care System, Seattle, Washington, USA. VA Puget Sound Health Care System, Building 1/Room 517, 1660 So. Columbian Way, Mail Stop S-151, Seattle, WA 98108 USA

## Abstract

Astrocytes respond to multiple forms of central nervous system (CNS) injury by entering a reactive state characterized by morphological changes and a specific pattern of altered protein expression. Termed astrogliosis, this response has been shown to strongly influence the injury response and functional recovery of CNS tissues. This pattern of CNS inflammation and injury associated with astrogliosis has recently been found to occur in the energy homeostasis centers of the hypothalamus during diet-induced obesity (DIO) in rodent models, but the characterization of the astrocyte response remains incomplete. Here, we report that astrocytes in the mediobasal hypothalamus respond robustly and rapidly to purified high-fat diet (HFD) feeding by cleaving caspase-3, a protease whose cleavage is often associated with apoptosis. Although obesity develops in HFD-fed rats by day 14, caspase-3 cleavage occurs by day 3, prior to the development of obesity, suggesting the possibility that it could play a causal role in the hypothalamic neuropathology and fat gain observed in DIO. Caspase-3 cleavage is not associated with an increase in the rate of apoptosis, as determined by TUNEL staining, suggesting it plays a non-apoptotic role analogous to the response to excitotoxic neuron injury. Our results indicate that astrocytes in the mediobasal hypothalamus respond rapidly and robustly to HFD feeding, activating caspase-3 in the absence of apoptosis, a process that has the potential to influence the course of DIO.

### Keywords

glia; astrocytes; apoptosis; obesity; neuron injury; hypothalamus



**Corresponding author:** Joshua P. Thaler UW medicine at South Lake Union, 850 Republican St, Box 358055, Seattle, WA 98109. Ph: (206) 897-1802, Fax: (206) 897-5293, jpthaler@uw.edu.

## 1. INTRODUCTION

Astrocytes are the most abundant cell type in the central nervous system (CNS), where they play many important roles, including providing structural support, supplying energy to neurons in the form of lactate, participating in the function of the blood-brain barrier, buffering extracellular neurotransmitters and ions, and in some cases modulating synaptic transmission (Wang and Bordey, 2008). Astrocytes are also an integral component of the CNS response to injurious stimuli such as stroke, physical trauma, tumors, hypoxia, infection, neurodegenerative disease, and excitotoxicity. In response to these stimuli, astrocytes enter a reactive state, characterized by increases in cell number, cell size, and other morphological changes associated with increased expression of the cytoskeletal intermediate filament proteins vimentin, nestin, and glial fibrillary acidic protein (GFAP) (Ridet et al., 1997). Reactive astrogliosis is characteristic of CNS injury, and can be evoked by insults that specifically target neurons as well as by more generalized damage (Acarin et al., 2005; Pekny and Nilsson, 2005).

Reactive astrocytes are hypothesized to alter the course of CNS injury, but whether they restrain or promote neuronal damage appears to be context-dependent. For example, combined deficiency of vimentin and GFAP, which impairs astrocyte activation, increases ischemic damage following cerebral artery occlusion (Li et al., 2008). Similarly, selective ablation of reactive astrocytes increases the severity of spinal cord and cortical injury (Faulkner et al., 2004; Myer et al., 2006). In contrast, over longer periods of time reactive astrocytes can also impair the function of local neurons, limit axonal and synaptic regeneration, and restrain neurogenesis in old mice (Larsson et al., 2004; Menet et al., 2003; Wilhelmsson et al., 2004). It has been suggested that reactive astrocytes are typically protective in the short-term response to acute injury, but can be detrimental to recovery in conditions of chronic injury, neurodegeneration, and aging (Pekny and Nilsson, 2005); however the role of astrogliosis may also be context-dependent.

In rodents, purified high-fat diet (HFD) consumption rapidly induces inflammatory signaling and markers of neuron injury in the mediobasal hypothalamus, responses that are accompanied by reactive astrogliosis (Horvath et al., 2010; Thaler et al., 2012). Prolonged HFD exposure is also associated with a 25% reduction in pro-opiomelanocortin (POMC) neurons (Thaler et al., 2012), an anorexigenic cell population important for body fat mass regulation. While the mechanism for POMC neuron loss is not yet established, a large increase in apoptosis in the hypothalamus of HFD-fed rats has been reported (Moraes et al., 2009), although recent work in mice failed to replicate this finding (McNay et al., 2012), raising doubts about the universality of this phenomenon. Moreover, neither study examined hypothalamic apoptosis during the first week of HFD feeding before significant body fat accumulation, leaving unanswered the question of whether observed patterns of apoptosis could be causally related to the obese phenotype.

Caspase-3 is an executioner caspase whose activation by proteolytic cleavage often plays a role in apoptosis (Earnshaw et al., 1999). In some cell types, however, caspase-3 activation plays non-apoptotic roles, including in cell differentiation, cell cycle regulation, and cell migration (Schwerk and Schulze-Osthoff, 2003; Zhao et al., 2006). In the CNS, caspase-3 participates in cytoskeletal remodeling in neurons and astrocytes (Acarin et al., 2007; Rohn et al., 2004) and in the differentiation of astrocyte subpopulations (Oomman et al., 2006). Neuron injury resulting from excessive stimulation by the excitatory neurotransmitter glutamate (termed “excitotoxicity”) causes widespread activation of caspase-3 (Acarin et al., 2005; Acarin et al., 2007; Narkilahti et al., 2003; Villapol et al., 2008), in part in neurons undergoing apoptosis, but primarily in the nuclei of astrocytes that are not undergoing apoptosis. In the context of excitotoxicity, caspase-3 activation is thought to play a role in

the cytoskeletal remodeling that accompanies astrogliosis in response to neuron injury (Villapol et al., 2008). In addition, recent evidence suggests caspase activation in astrocytes may be required for the full expression of the reactive phenotype (Aras et al., 2012).

Given the importance of astrocyte responses to neuron injury, and the evidence of hypothalamic neuron injury during HFD feeding, we sought to further characterize the astrocyte phenotype in this context. We hypothesized that HFD feeding induces activated caspase-3 immunoreactivity in astrocytes without provoking apoptosis, a sign of an astroglial response to CNS injury. To test this hypothesis, we maintained rats on an *ad libitum* HFD feeding regimen for 1, 3, 7 or 14 days, and determined the CNS expression of active (cleaved) caspase-3 in astrocytes and neurons. To test whether caspase-3 activation in this context is associated with apoptosis, we also performed terminal dUTP nick end labeling (TUNEL) staining.

## 2. RESULTS

### 2.1. Body Composition of HFD-fed Rats

Rats were switched from standard chow to HFD (Research Diets D12492) and sacrificed after 1, 3, 7, or 14 days of HFD exposure (n = 5, 6, 6, 4 rats, respectively). Body composition determined by quantitative magnetic resonance at the beginning and end of the HFD intervention revealed increases in total fat mass (Figure 1A) and fat mass accumulation over the course of HFD feeding (Figure 1B) that were proportional to the duration of HFD exposure. In contrast, lean mass did not differ between groups (Figure 1C). As reported previously (Thaler et al., 2012), rats were hyperphagic during the first week of HFD exposure (data not shown). As expected, rats increased energy intake and gained fat rapidly following the switch to a HFD.

### 2.2. Distribution and Timecourse of Cleaved Caspase-3 Immunoreactivity in the CNS of HFD-fed Rats

Specificity and sensitivity of the cleaved caspase-3 antibody were confirmed using a blocking peptide and a positive control of human tonsil tissue (Figure 2A and 2B; tonsil data not shown). Cleaved caspase-3 immunoreactivity was observed in ARC, VMH and primary somatosensory (S1) cortex at all time points in both chow- and HFD-fed rats, compared to sections treated with a blocking peptide (representative images in Figure 2). However, staining was considerably fainter in the chow and 1-d HFD conditions than at other time points (compare Figures 2D–2F to 2G–2L). During HFD feeding, cleaved caspase-3 immunoreactivity in the ARC increased both in intensity and quantity, peaking at 3–7 d and declining at 14 d (Figure 2, 3A). The increase in discrete caspase-3 immunoreactive cells was statistically significant at 3 and 7 d relative to chow (Figure 3A; $p<0.001$). A similar pattern was observed in both S1 cortex and VMH (Figure 3B, C; data not shown). Thus, HFD feeding is associated with a rapid induction of caspase-3 activation in hypothalamic and extrahypothalamic regions of the CNS.

### 2.3. Double Immunohistochemical Localization of Cleaved Caspase-3 Immunoreactivity with Cell Type-specific Markers

To identify the specific cell types involved in the caspase-3 response to HFD feeding, we performed double-label immunofluorescence analysis of the 3-d HFD time point because it was associated with the greatest degree of cleaved caspase-3 immunoreactivity in the ARC (Figure 2G and 3A). Using NeuN and GFAP immunoreactivity as a marker for neurons and astrocytes, respectively, we observed little association between neurons and caspase-3 immunoreactivity (3.6%; Figure 4A and 4B; quantified in 4E). In contrast, nearly all cleaved caspase-3 immunoreactivity was present in the nuclei of GFAP-positive cells (92.5%; Figure

4C and 4D; DAPI staining not shown; quantified in 4E). The disparity between cleaved caspase-3 localization in neurons and astrocytes was highly significant (Figure 4E; $p < 0.001$). Astrocytes displaying cleaved caspase-3 immunoreactivity did not exhibit morphological evidence of apoptosis (e.g. fragmented processes and pyknotic nuclei) in either cell type. These findings indicate that caspase-3 activation in this context occurs primarily in astrocytes, with little evidence for activation in neurons.

### 2.4. Apoptosis in the CNS of HFD-fed Rats

To determine whether caspase-3 activation was associated with increased apoptosis in the hypothalamus, we performed TUNEL staining on sections from rats fed chow or HFD for 3 d, 7 d, or 3 mo. In contrast with one prior report (Moraes et al., 2009), we observed few TUNEL-positive cells in the ARC and VMH of chow or HFD-fed rats at all time points despite obtaining clear TUNEL staining in three positive control conditions (DNase I-treated brain tissue, spleen, and brain tissue from colchicines-treated rats; Figure 5 A, 5B; colchicine data not shown). Quantification of TUNEL-positive cell number revealed no statistically significant differences between groups (ARC TUNEL+ cells per section for chow, HFD 3d, HFD 7d, HFD 3m: 0.17, 0.00, 0.05, 0.25; VMH TUNEL+ cells per section for chow, HFD 3d, HFD 7d, HFD 3m: 0.05, 0.04, 0.00, 0.04; n = 5, 6, 6, 4 respectively, representative images Figure 5C–F). Given the nearly three order of magnitude difference between cleaved caspase-3 immunoreactivity (80–100 cells/section) and TUNEL positivity (0–0.25 cells/section), HFD-induced caspase-3 activation in astrocytes is largely independent of apoptosis, consistent with previous reports of non-apoptotic activation of astrocytes in the context of neuron injury (Acarin et al., 2005; Acarin et al., 2007; Narkilahti et al., 2003; Villapol et al., 2008).

## 3. DISCUSSION

Our findings indicate that HFD feeding causes a substantial and widespread activation of caspase-3 in the nuclei of astrocytes of the rat brain, including in the energy homeostasis centers of the MBH, with little evidence of caspase-3 activation in neurons. This increase was evident at 3 days, persisted at day 7, and began to wane by day 14. The maximal increment of cleaved caspase-3 immunoreactivity in the ARC occurred on day 3, after only a small increase of fat mass, suggesting that the response precedes and is therefore not dependent on the development of obesity. However, we found no evidence of increased apoptosis in the brains of HFD-fed rats at any time point, consistent with a role for caspase-3 activation in non-apoptotic processes such as cell differentiation, cell cycle regulation, cell migration, and cytoskeletal remodeling (Acarin et al., 2007; Rohn et al., 2004; Schwerk and Schulze-Osthoff, 2003; Zhao et al., 2006). These findings are compatible with previous reports of rapid-onset CNS injury responses during HFD feeding, and reinforce the possibility that astrocytes participate in this process. Although astrocytes play a protective role in the acute response to multiple forms of CNS injury (Faulkner et al., 2004; Li et al., 2008; Myer et al., 2006), the extent to which astrogliosis in this context is beneficial, neutral or harmful awaits further study.

The observation that astrocyte caspase-3 activation diminishes by day 14 of HFD feeding suggests a dynamic CNS response to injury. This pattern mirrors that of increased inflammatory gene expression and reactive astrogliosis in the hypothalamus of HFD-fed rats, which develop as early as day 1, diminish to baseline levels over the next few weeks, and return again with prolonged HFD feeding (Thaler et al., 2012). These similarities raise the testable possibility that the caspase response is not transient–as would be the case with successful restoration of CNS homeostasis—but rather may recur with established obesity in parallel with astrocyte activation and inflammatory signaling.

In a previous study, we identified multiple signs of MBH neuron injury in rodents fed HFD, but other brain regions were not as thoroughly assessed (Thaler et al., 2012). While the microglial accumulation and gliosis we observed were most apparent in the ARC of HFD-fed rodents and MBH of obese humans, our present results suggest that at least the astrocyte response to HFD feeding may be more widespread, a result consistent with observations of increased inflammatory gene expression in the hippocampus and cortex of HFD-fed rodents (Jeon et al., 2012; Zhang et al., 2005). Alternatively, caspase 3 activation in astrocytes may represent a distinct HFD-induced alteration of CNS homeostasis that occurs broadly in the CNS. In either case, HFD feeding likely represents a general CNS insult with differential regional susceptibility to injury. As an area of minimal blood-brain barrier protection, the ARC may receive more sustained and severe exposure, resulting in more substantial neurotoxicity. Determining the validity of this hypothesis awaits a better understanding of the mechanisms underlying HFD-induced neuron injury.

Additional work is needed to determine the precise role played by caspase-3 in reactive astrocytes in this setting and the significance of its nuclear localization in these cells. Depending on the cell type and stimulus, activated caspase-3 can occur in the cytoplasm, neuronal processes, and/or nucleus (Acarin et al., 2007; Su et al., 2001). Nuclear localization of caspase-3 in astrocytes has been previously reported in models of neuron injury (Acarin et al., 2007). During apoptosis, caspase-3 cleaves a variety of nuclear substrates, including Poly(ADP-ribose) Polymerase-1, acinus, and lamins (Eldadah and Faden, 2000). In the current context, caspase-3 activation could play a role in modulating nuclear proteins involved in inflammatory signaling (Lamkanfi et al., 2006; Petrilli et al., 2004), transcriptional regulation (Lamkanfi et al., 2006), and cytoskeletal elements (Acarin et al., 2007) that are involved in astrocyte activation.

Under basal (or “resting”) conditions, astrocytes are characterized by multiple long, thin cellular processes that do not overlap with those of neighboring astrocytes. Upon CNS injury, astrocytes enter a reactive state, undergoing a remodeling process that results in general cellular hypertrophy and thickened processes that overlap with neighboring astrocytes, ultimately forming a network or “syncytium”. Previous studies have found that this reactive gliosis is associated with caspase-3 activation in the setting of CNS injury such as excitotoxicity and trauma (Acarin et al., 2005; Acarin et al., 2007; Beer et al., 2000; Narkilahti et al., 2003; Villapol et al., 2008). For example, Acarin et al. reported astrogliosis and glial caspase-3 activation in response to excitotoxic neuron injury caused by NMDA injection into the cortex of 9-day-old rat pups, despite no evidence of astrocyte apoptosis, echoing a previous study examining seizure-induced caspase-3 activation by Narkilahti et al. (Acarin et al., 2005; Narkilahti et al., 2003). Further temporal characterization of the astrocyte response to excitotoxic injury revealed a rapid induction of cleaved caspase-3 immunoreactivity within four hours, followed by a steady decline through 14 days post-injury (Acarin et al., 2007). In this model, astrocyte caspase-3 activation was observed in response to neuronal injury without associated apoptosis. Beer et al. observed a similar activation of astrocyte caspase-3 in the context of traumatic injury of the cortex, although the association of caspase-3 activation with apoptosis in astrocytes was not quantified (Beer et al., 2000).

These observations raise the important question of how cells activate caspase-3 without triggering apoptosis. Without a direct assessment of *in vivo* caspase enzymatic function, we cannot exclude the possibility that the level of activation was insufficient to trigger apoptotic pathways. Alternatively, the presence of anti-apoptotic proteins may inhibit the cleavage of apoptotic substrates by caspase-3. Notably, Villapol et al. found that along with cleaved caspase-3, astrocytes in the cortex of NMDA-treated rat pups co-express several proteins known to inhibit apoptosis, including survivin and HSP25/27 (Villapol et al., 2008). Using a

similar experimental design, Acarin et al. detected caspase-3 cleaved GFAP in cortical astrocytes following excitotoxic injury, suggesting that the co-expression of anti-apoptotic proteins may channel the activity of caspase-3 away from apoptosis and toward the cytoskeletal remodeling processes that are integral to astrogliosis (Acarin et al., 2007).

Based on these considerations, we interpret our observation of widespread caspase-3 cleavage in astrocytes as a feature of the astrocyte response to CNS injury induced by HFD feeding, rather than as apoptosis. We further speculate that the activation of caspase-3 in this context plays a role in the cytoskeletal remodeling processes involved in astrogliosis. Close parallels between our findings and those of astrocytes responding to excitotoxic damage raise the interesting possibility that excitotoxicity contributes to CNS injury during HFD feeding. This is consistent with the fact that exposure to palatable energy-dense food increases the activity of anorexigenic POMC neurons, presumably as a counterregulatory response to maintain energy homeostasis (Shu et al., 2003). Combined with the finding of gliosis in the MBH of obese humans (Thaler et al., 2012), these results justify future research on the possible role of excitotoxicity in obesity-associated neuronal injury and the potential contribution of astrogliosis to the hypothalamic dysfunction underlying obesity pathogenesis.

A growing body of evidence implicates MBH inflammatory signaling and neuron injury in the pathogenesis of obesity (De Souza et al., 2005; Kleinridders et al., 2009; Thaler et al., 2012; Zhang et al., 2008). In rodents, neuronal inflammatory signaling is rapidly induced by HFD feeding and is required for the full development of DIO (De Souza et al., 2005; Kleinridders et al., 2009; Zhang et al., 2008). Inflammatory signaling in the MBH is also accompanied by markers of neuron injury and possibly apoptosis under certain conditions (McNay et al., 2012; Moraes et al., 2009). In humans, obesity is associated with radiographic evidence of gliosis in the MBH (Thaler et al., 2012), raising the possibility that neuron injury contributes to the establishment and/or defense of an elevated fat mass. Our findings demonstrate that astrocytes react rapidly to HFD feeding by activating caspase-3 in the absence of apoptosis, adding to the evidence for rapid-onset CNS injury upon obesogenic diet exposure. This occurs prior to the development of obesity, suggesting that it is not secondary to the obese state. Since astrocytes modulate CNS responses to injurious stimuli, this phenomenon has the potential to play a role in the hypothalamic dysfunction that contributes to the development and maintenance of obesity.

## 4. EXPERIMENTAL PROCEDURES

### Animals

Weight-matched male Wistar rats (300–350 g; Harlan) were housed individually in a specific pathogen-free environment, maintained in a temperature-controlled room with a 12:12-h light-dark cycle, and provided with *ad libitum* access to water and either standard laboratory chow or HFD for periods ranging from 1 to 14 days. Standard laboratory chow was LabDiet 5001, an unpurified 12% fat diet composed primarily of corn and soybean meal, with a physiological fuel value of 3.34 kcal/g. Research Diets D12492 is a purified high-fat diet with 60% kcal as fat (90% lard, 10% soybean oil; 32% saturated, 36% monounsaturated; 32% polyunsaturated; 14:1 n-6:n-3 ratio) and a physiological fuel value of 5.24 kcal/g. All study protocols involving rats were approved by the Institutional Animal Care and Use Committee at the University of Washington and conducted in accordance with the National Institutes of Health guidelines for the care and use of animals.

### Body Composition

Determinations of body lean mass, fat mass and water content were made in conscious rats using quantitative magnetic resonance (EchoMRI 3-in-1 machine whole body composition analyzer; Echo Medical Systems, Houston, TX).

### Immunohistochemistry and TUNEL Staining

Animals were perfused and fixed with cold PBS followed by 4% paraformaldehyde/PBS. Brains were collected and cryoprotected using 25% sucrose in PBS, and 14μm-thick frozen sections were generated in the coronal plane through the rat hypothalamus (at the level of the medial ARC; region of interest bregma −2.8 to −3.1 mm). For fluorescent staining, sections were blocked in 5% normal goat or donkey serum (Jackson ImmunoResearch Laboratories Inc.), and incubated overnight at 4°C with mouse anti-GFAP (1:10,000; Sigma-Aldrich C9205), mouse NeuN (1:1,000; Chemicon MAB377), or rabbit polyclonal cleaved caspase-3 antibody (1:1,000; Cell Signaling 9661). Immunofluorescence was performed with a combination of Alexa Fluor 488– or Alexa Fluor 594–labeled anti rabbit or anti mouse secondary antibodies (1:500; Invitrogen) and DAPI (Sigma-Aldrich) to identify cell nuclei. NeuN antibodies have been widely validated in the literature as a neuronal marker (Mullen et al., 1992; Wolf et al., 1996), and GFAP is widely considered a marker of astrocytes, particularly in the reactive state (Wolf et al., 1996). In addition, we observed no overlap between these two markers.

For the immunohistochemical detection of cleaved caspase 3 immunoreactivity, slides were briefly immersed in PBS containing 5% BSA (bovine serum albumin), 5% normal goat serum (NGS) and 0.3% Triton x-100, followed by rabbit polyclonal cleaved caspase-3 antibody (Cell Signaling 9661) diluted 1:800 in PBS containing 1% BSA for 22 hr. at room temperature. This antibody recognizes the large fragment (17/19 kDa) of caspase-3 resulting from cleavage adjacent to Asp175 during conversion from proenzyme to active enzyme, and does not recognize full-length caspase-3. After this incubation, tissue sections were rinsed in PBS and immersed in biotinylated goat anti-rabbit IgG (1:600) in PBS for 70 min at room temperature, followed by 1:600 Elite ABC reagent (Vector Laboratories) in PBS for 60 min. Immunoreactivity was visualized by immersion in 0.05% diaminobenzidine (DAB) (Sigma cat. # D5905-100TAB) containing 0.01% hydrogen peroxide in 0.05 M Tris-HCl, pH 7.4 for 6 min. Slides were permanently mounted after dehydration with ethanol and cleared with xylene, and cover-slipped with Permaslip (American Master Tech, item# MMP0133). Controls included hypothalamus sections incubated with 2 parts of antibody and 1 part of cleaved caspase-3 Asp175 blocking peptide (Cell Signaling 1050), and human tonsil tissue as a positive control.

TUNEL staining was performed using the ApopTag Plus fluorescein in situ apoptosis detection kit (Chemicon; S7111). Sections were permeabilized using 2:1 ethanol:acetic acid at −20°C for 5 min followed by the standard protocol described in the included instruction manual. DNase I treated-sections of normal rat hypothalamus were used as a positive control. Briefly, sections were preincubated in DNase I buffer (30 mM Trizma base, pH 7.2, 4 mM $MgCl_2$, 0.1 mM DTT), treated for 10 minutes with DNase I (Sigma D7291; 8,000 U/mL; in DNase I buffer), rinsed 5 times in PBS, and processed for TUNEL staining as above.

### Image Capture and Quantification

Images were captured on an Eclipse E600 upright microscope equipped with a color digital camera (Nikon). All images were captured in JPEG format using the same capture settings, and were not subjected to any form of image processing before scoring. Representative images displayed in figures were subjected to contrast enhancement that was applied identically to all images within a figure. Quantification was performed in a blinded fashion

on anatomically matched brain regions (bregma −2.8 to −3.1 mm). Both sides of bilateral structures (e.g., ARC, VMH, etc.) were counted on 2 slides per animal (representing 4 brain sections), and replicate values from each animal were individually averaged before determining group means ($n$ = 5–8/group). Cell or puncta (small, discrete regions of staining) number was counted manually within prespecified regions of interest (ROIs) in the ARC, VMH, and S1 cortex using Photoshop (Adobe). For the ARC, the ROI approximated the entirety of the nucleus, while for the larger VMH and S1 cortex, a square ROI (0.4 mm X 0.4 mm) was used. For determining the double immunohistochemical localization of caspase-3 puncta with NeuN or GFAP immunoreactivity, dual fluorescence images were analyzed within the ARC ROI.

### Statistical Analysis

All results are expressed as mean ± SEM. Statistical analyses were performed using Graph Pad PRISM (version 4.0b; Graph Pad Software). One-way ANOVA with Tukey post hoc test was used to compare mean values among multiple groups. Two-group comparisons were assessed by unpaired or paired two-tailed Student's t-test. In all instances, P values of $<0.05$ were considered statistically significant.

## Acknowledgments

This work was supported by a National Institutes of Health (NIH) Fellowship Training Program Award (T32DK007247), an NIH National Research Service Award (F32DK091989) to S.G., an NIH Career Development Award (DK088872), an NIH-funded Diabetes Research Center Pilot and Feasibility award (DK017047) to J.T., the NIH-funded University of Washington Nutrition Obesity Research Center and Diabetes Research Center (grant P30DK017047 to D.B.), and NIH Grants DK068384, DK083042, and DK052989 (to M.S.).

This work was also supported by resources from the Office of Research and Development, Medical Research Service, Department of Veterans Affairs, including the Merit Review Research Program and the Research Enhancement Award Program. D.B. is the recipient of a Department of Veterans Affairs Senior Research Career Scientist Award at the Veterans Affairs Puget Sound Health Care System.

Additional support came from the biomedical research core programs Cellular and Molecular Imaging Core of the University of Washington NIH/NIDDK Diabetes Research Center.

Alan Gown (Phenopath Labs, Seattle) provided human tonsil tissue as a positive control for TUNEL staining. Miles Matsen, Loan Nguyen, Kayoko Ogimoto, and Alex Cubelo provided technical assistance.

## Abbreviations

| | |
|---|---|
| **CNS** | Central nervous system |
| **DIO** | Diet induced obesity |
| **HFD** | Purified high fat diet |
| **GFAP** | Glial fibrillary acidic protein |
| **POMC** | Pro-opiomelanocortin |
| **TUNEL** | Terminal dUTP nick end labeling |
| **ARC** | Arcuate nucleus |
| **VMH** | Ventromedial hypothalamus |
| **MBH** | Mediobasal hypothalamus |
| **NMDA** | N-methyl-D-aspartate |

## REFERENCES


Acarin L, et al. Astroglial nitration after postnatal excitotoxic damage: correlation with nitric oxide sources, cytoskeletal, apoptotic and antioxidant proteins. J Neurotrauma. 2005; 22:189–200. [PubMed: 15665612]

Acarin L, et al. Caspase-3 activation in astrocytes following postnatal excitotoxic damage correlates with cytoskeletal remodeling but not with cell death or proliferation. Glia. 2007; 55:954–965. [PubMed: 17487878]

Aras R, Barron AM, Pike CJ. Caspase activation contributes to astrogliosis. Brain Res. 2012; 1450:102–115. [PubMed: 22436850]

Beer R, et al. Temporal profile and cell subtype distribution of activated caspase-3 following experimental traumatic brain injury. J Neurochem. 2000; 75:1264–1273. [PubMed: 10936210]

De Souza CT, et al. Consumption of a fat-rich diet activates a proinflammatory response and induces insulin resistance in the hypothalamus. Endocrinology. 2005; 146:4192–4199. [PubMed: 16002529]

Earnshaw WC, Martins LM, Kaufmann SH. Mammalian caspases: structure, activation, substrates, and functions during apoptosis. Annu Rev Biochem. 1999; 68:383–424. [PubMed: 10872455]

Eldadah BA, Faden AI. Caspase pathways, neuronal apoptosis, and CNS injury. J Neurotrauma. 2000; 17:811–829. [PubMed: 11063050]

Faulkner JR, et al. Reactive astrocytes protect tissue and preserve function after spinal cord injury. J Neurosci. 2004; 24:2143–2155. [PubMed: 14999065]

Horvath TL, et al. Synaptic input organization of the melanocortin system predicts diet-induced hypothalamic reactive gliosis and obesity. Proc Natl Acad Sci U S A. 2010; 107:14875–14880. [PubMed: 20679202]

Jeon BT, et al. Resveratrol attenuates obesity-associated peripheral and central inflammation and improves memory deficit in mice fed a high-fat diet. Diabetes. 2012; 61:1444–1454. [PubMed: 22362175]

Kleinridders A, et al. MyD88 signaling in the CNS is required for development of fatty acid-induced leptin resistance and diet-induced obesity. Cell Metab. 2009; 10:249–259. [PubMed: 19808018]

Lamkanfi M, et al. Caspases leave the beaten track: caspase-mediated activation of NF-kappaB. J Cell Biol. 2006; 173:165–171. [PubMed: 16618810]

Larsson A, et al. Increased cell proliferation and neurogenesis in the hippocampal dentate gyrus of old GFAP(−/−)Vim(−/−) mice. Neurochem Res. 2004; 29:2069–2073. [PubMed: 15662841]

Li L, et al. Protective role of reactive astrocytes in brain ischemia. J Cereb Blood Flow Metab. 2008; 28:468–481. [PubMed: 17726492]

McNay DE, et al. Remodeling of the arcuate nucleus energy-balance circuit is inhibited in obese mice. J Clin Invest. 2012; 122:142–152. [PubMed: 22201680]

Menet V, et al. Axonal plasticity and functional recovery after spinal cord injury in mice deficient in both glial fibrillary acidic protein and vimentin genes. Proc Natl Acad Sci U S A. 2003; 100:8999–9004. [PubMed: 12861073]

Moraes JC, et al. High-fat diet induces apoptosis of hypothalamic neurons. PLoS One. 2009; 4:e5045. [PubMed: 19340313]

Mullen RJ, Buck CR, Smith AM. NeuN, a neuronal specific nuclear protein in vertebrates. Development. 1992; 116:201–211. [PubMed: 1483388]

Myer DJ, et al. Essential protective roles of reactive astrocytes in traumatic brain injury. Brain. 2006; 129:2761–2772. [PubMed: 16825202]

Narkilahti S, et al. Expression and activation of caspase 3 following status epilepticus in the rat. Eur J Neurosci. 2003; 18:1486–1496. [PubMed: 14511328]

Oomman S, et al. Bergmann glia utilize active caspase-3 for differentiation. Brain Res. 2006; 1078:19–34. [PubMed: 16700096]

Pekny M, Nilsson M. Astrocyte activation and reactive gliosis. Glia. 2005; 50:427–434. [PubMed: 15846805]

Petrilli V, et al. Noncleavable poly(ADP-ribose) polymerase-1 regulates the inflammation response in mice. J Clin Invest. 2004; 114:1072–1081. [PubMed: 15489954]

Ridet JL, et al. Reactive astrocytes: cellular and molecular cues to biological function. Trends Neurosci. 1997; 20:570–577. [PubMed: 9416670]

Rohn TT, et al. Caspase activation independent of cell death is required for proper cell dispersal and correct morphology in PC12 cells. Exp Cell Res. 2004; 295:215–225. [PubMed: 15051504]

Schwerk C, Schulze-Osthoff K. Non-apoptotic functions of caspases in cellular proliferation and differentiation. Biochem Pharmacol. 2003; 66:1453–1458. [PubMed: 14555221]

Shu IW, et al. The fatty acid synthase inhibitor cerulenin and feeding, like leptin, activate hypothalamic pro-opiomelanocortin (POMC) neurons. Brain Res. 2003; 985:1–12. [PubMed: 12957363]

Su JH, et al. Activated caspase-3 expression in Alzheimer's and aged control brain: correlation with Alzheimer pathology. Brain Res. 2001; 898:350–357. [PubMed: 11306022]

Thaler JP, et al. Obesity is associated with hypothalamic injury in rodents and humans. J Clin Invest. 2012; 122:153–162. [PubMed: 22201683]

Villapol S, et al. Survivin and heat shock protein 25/27 colocalize with cleaved caspase-3 in surviving reactive astrocytes following excitotoxicity to the immature brain. Neuroscience. 2008; 153:108–119. [PubMed: 18358624]

Wang DD, Bordey A. The astrocyte odyssey. Prog Neurobiol. 2008; 86:342–367. [PubMed: 18948166]

Wilhelmsson U, et al. Absence of glial fibrillary acidic protein and vimentin prevents hypertrophy of astrocytic processes and improves post-traumatic regeneration. J Neurosci. 2004; 24:5016–5021. [PubMed: 15163694]

Wolf HK, et al. NeuN: a useful neuronal marker for diagnostic histopathology. J Histochem Cytochem. 1996; 44:1167–1171. [PubMed: 8813082]

Zhang X, et al. High dietary fat induces NADPH oxidase-associated oxidative stress and inflammation in rat cerebral cortex. Exp Neurol. 2005; 191:318–325. [PubMed: 15649487]

Zhang X, et al. Hypothalamic IKKbeta/NF-kappaB and ER stress link overnutrition to energy imbalance and obesity. Cell. 2008; 135:61–73. [PubMed: 18854155]

Zhao X, et al. Caspase-3-dependent activation of calcium-independent phospholipase A2 enhances cell migration in non-apoptotic ovarian cancer cells. J Biol Chem. 2006; 281:29357–29368. [PubMed: 16882668]

- Purified high-fat diet feeding causes rapid caspase-3 activation in the CNS
- Activated caspase-3 is found almost exclusively in astrocytes
- Caspase-3 activation occurs in brain regions known to regulate energy balance
- Caspase-3 activation is not associated with an increase in apoptosis
- Astrocyte caspase-3 activation may reflect an astrocyte response to neuron injury

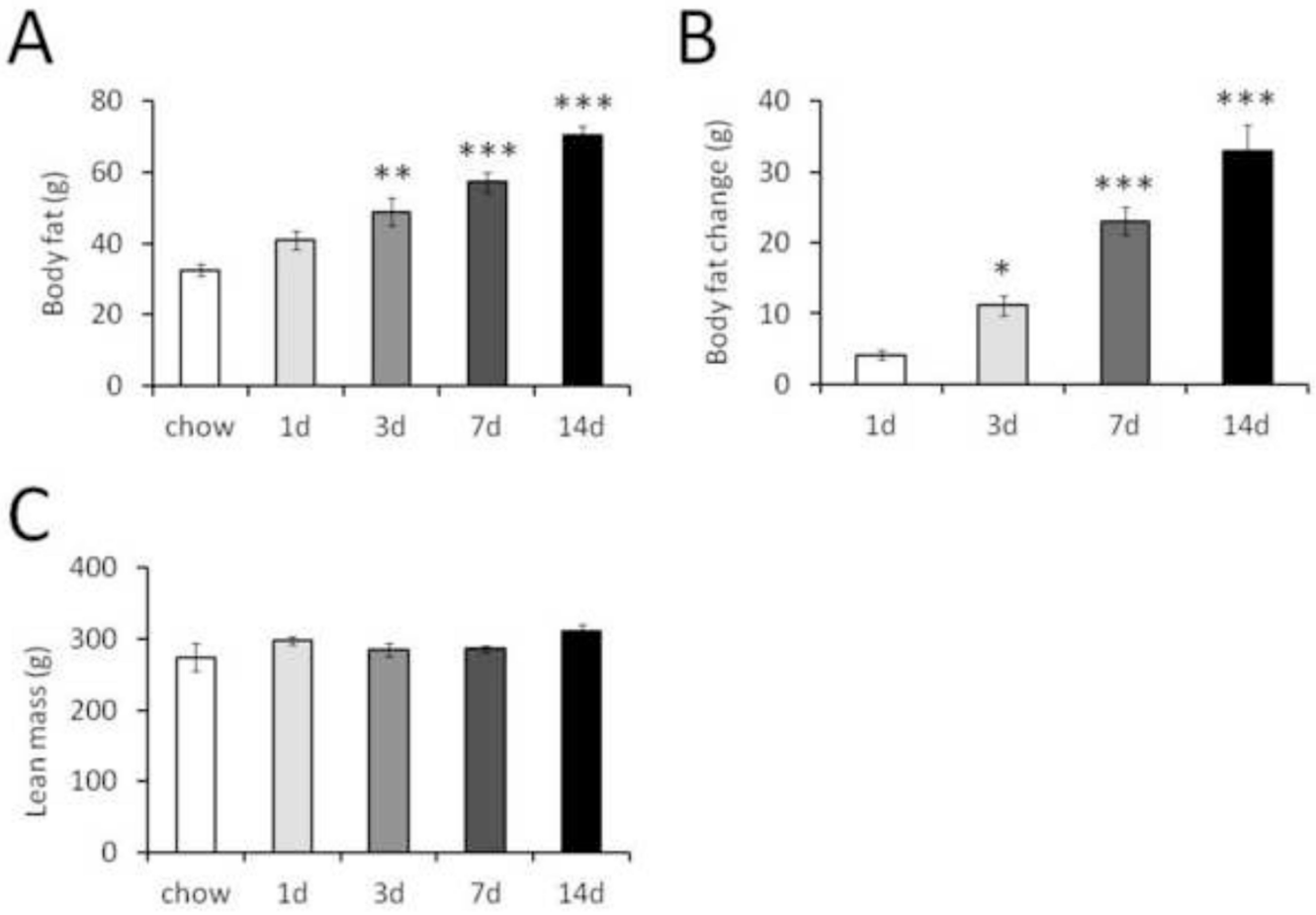


**Figure 1.**

Body composition of rats fed HFD. A, fat mass in rats after feeding chow or HFD for 1, 3, 7, or 14 days. B, change in fat mass (final minus initial) in rats fed HFD for 1, 3, 7, or 14 days. C, lean mass in rats after chow or HFD feeding for 1, 3, 7 or 14 days. n = 5, 6, 6, 4 rats, respectively. *, $p < 0.05$; **, $p < 0.01$; ***, $p < 0.001$ relative to chow or 1 d HFD by one-way ANOVA with Tukey post-test.

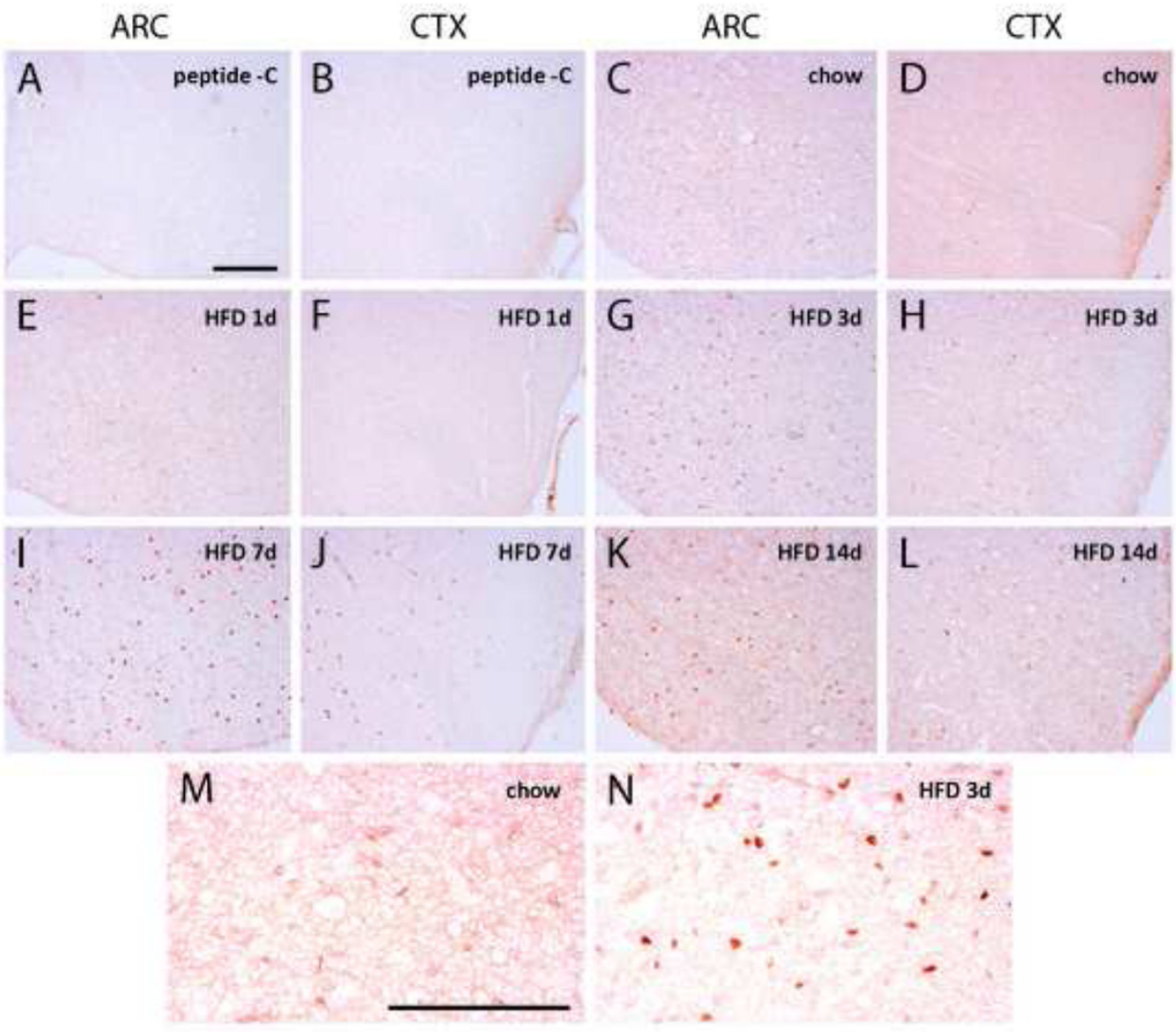


**Figure 2.**

Cleaved caspase-3 immunoreactivity in ARC and S1 cortex (coronal sections). Low-magnification representative images. A and B, ARC and S1 cortex with blocking peptide. C and D, ARC and S1 cortex in chow-fed rats. E and F, ARC and S1 cortex in 1 day HFD-fed rats. G and H, ARC and S1 cortex in 3 day HFD-fed rats. I and J, ARC and S1 cortex in 7 day HFD-fed rats. K and L, ARC and S1 cortex in 14 day HFD-fed rats. M, high-magnification of ARC in chow-fed rat. N, high-magnification of ARC in 3d HFD-fed rat. Scale bars represent 100 μM.

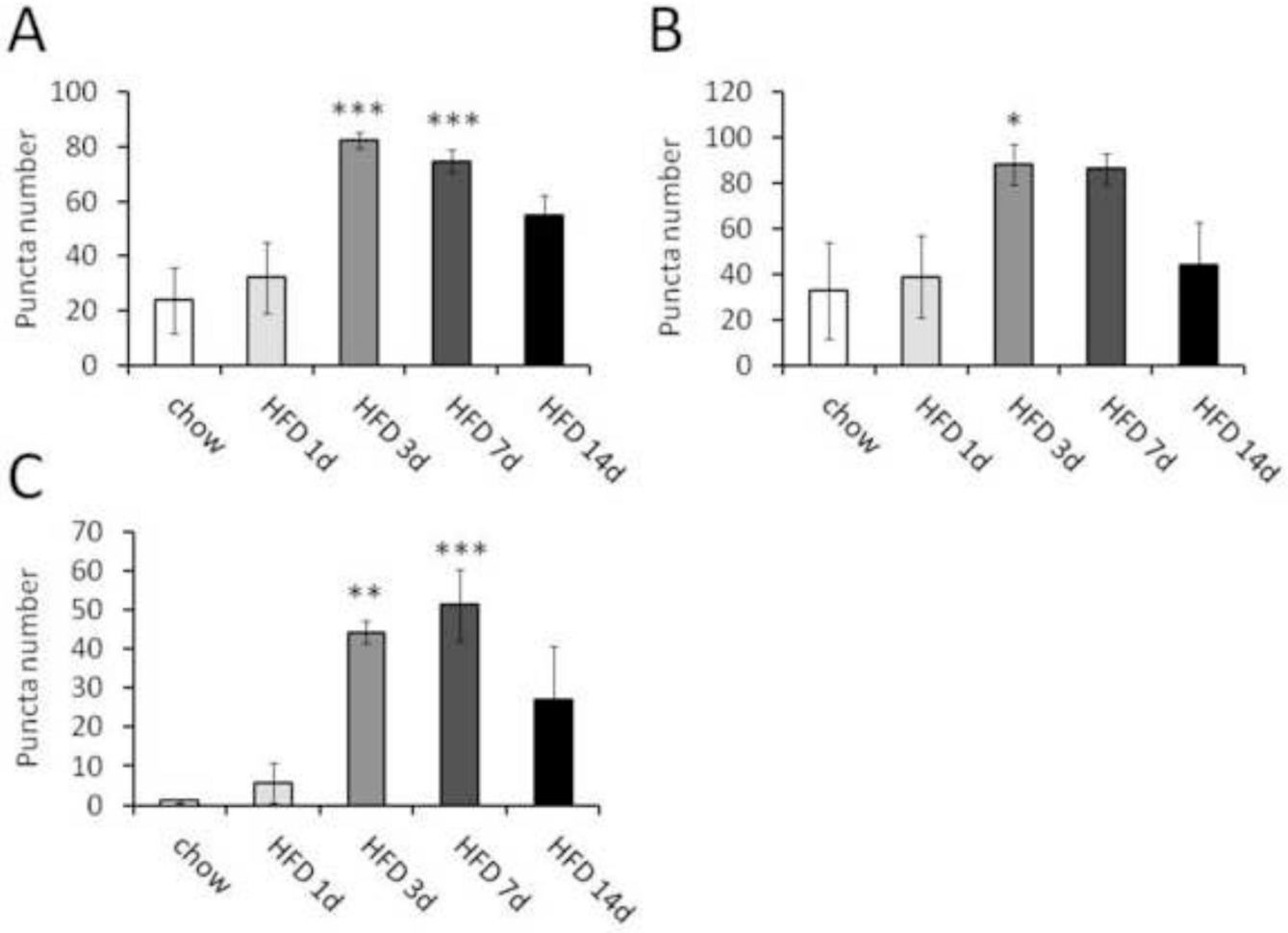


**Figure 3.**

Quantification of cleaved caspase-3 immunoreactivity in coronal sections of ARC, VMH and S1 cortex on day 1, 3, 7 or 14 of HFD feeding. A, ARC. B, VMH. C, S1 cortex. n = 5, 6, 6, 4 rats, respectively. *, $p < 0.05$; **, $p < 0.01$; ***, $p < 0.001$ relative to 1d HFD by ANOVA with Tukey post-test.

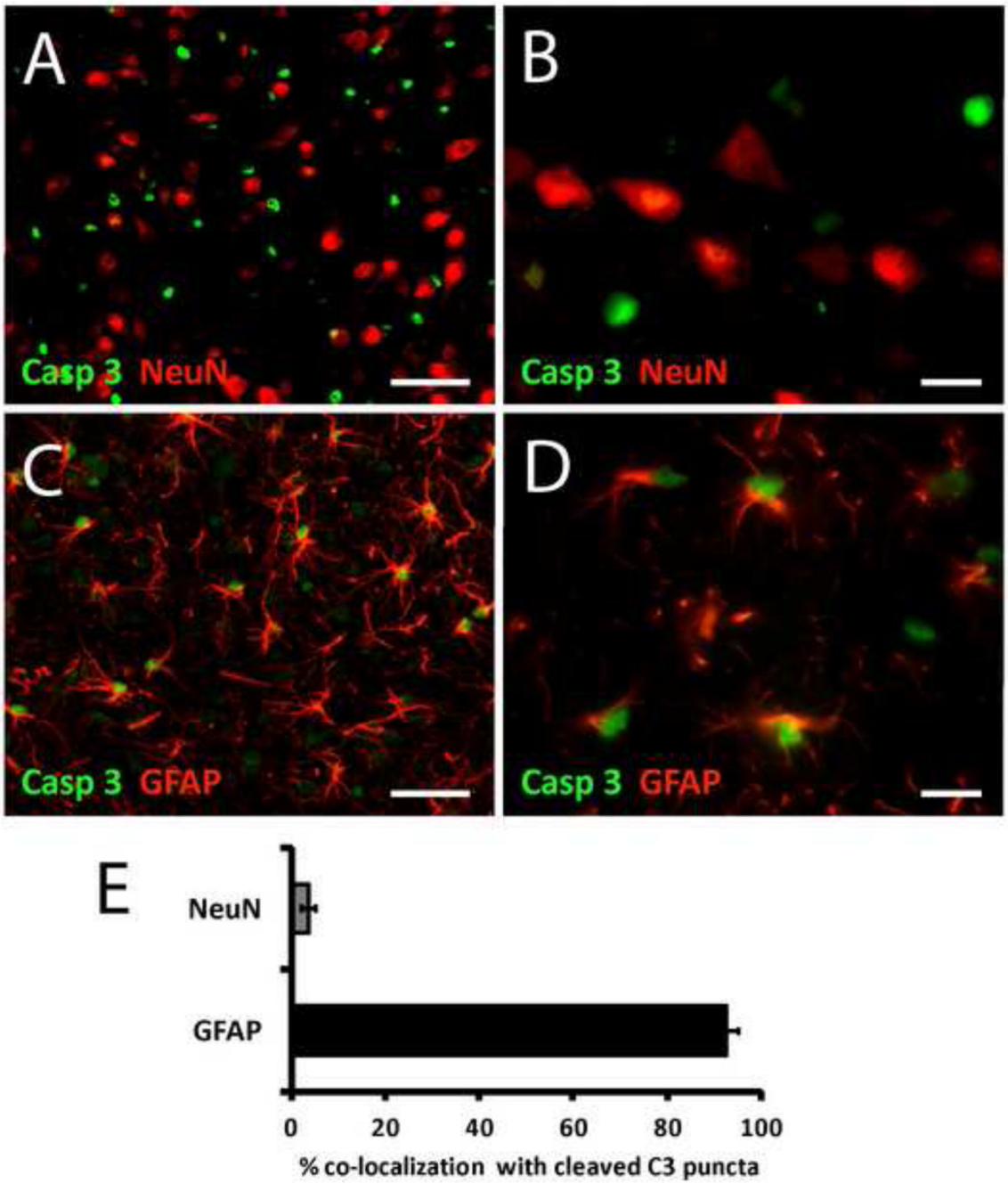


**Figure 4.**

Double immunohistochemical localization of NeuN and GFAP immunoreactivity with cleaved caspase-3 immunoreactivity in ARC of 3 day HFD-fed rats (coronal sections). A, low magnification image of cleaved caspase-3 (green) and NeuN (red). B, high magnification image of cleaved caspase-3 (green) and NeuN (red). C, low magnification image of cleaved caspase-3 (green) and GFAP (red). D, high magnification image of cleaved caspase-3 (green) and GFAP (red). E, quantification of double immunohistochemical localization of cleaved caspase-3 immunoreactivity with NeuN and GFAP ($p < 0.001$ by paired t-test). n = 5, 6, 6, 4 rats, respectively. Scale bar: A and C, 20 μM; B and D, 5μM.

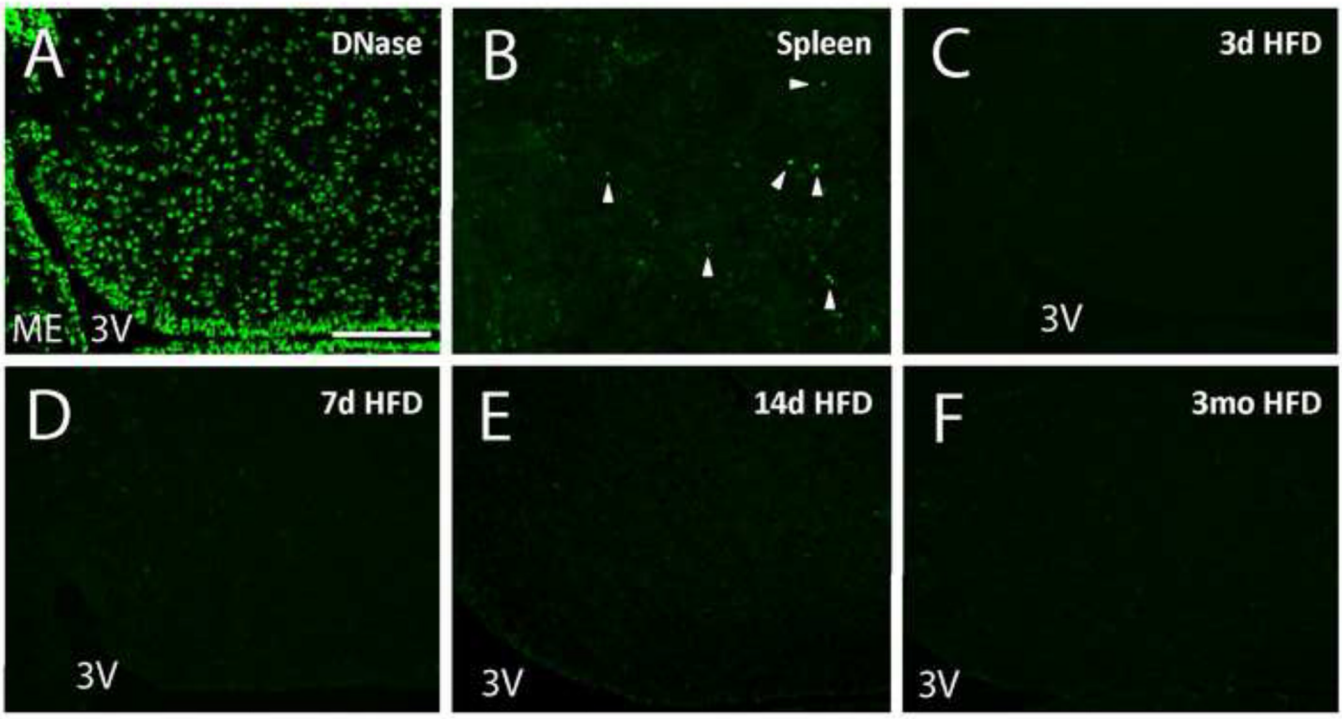


**Figure 5.**

TUNEL staining. A, DNase I-treated positive control section from a chow-fed rat, showing ARC. Area of ARC is outlined; median eminence and third ventricle indicated. Note large TUNEL-positive nuclei, which are characteristic of this positive control method, but distinct from the condensed (pyknotic) morphology observed in true apoptotic nuclei. B, rat spleen positive control, showing characteristic small pyknotic nuclei. C, representative ARC image from chow group. D, representative ARC image from 3 day HFD group. E, representative ARC image from 7 day HFD group. F, representative ARC image from 3 month group. Scale bars represent 100 μM. All images are coronal sections with the ventral surface to the left, and the third ventricle and median eminence marked (3V; ME).